Journal of Hazardous Materials 239–240 (2012) 78–87

Contents lists available at SciVerse ScienceDirect

Journal of Hazardous Materials

journal homepage: www.elsevier.com/locate/jhazmat

Polycyclic aromatic hydrocarbons in $PM_{2.5}$ in Guangzhou, southern China: Spatiotemporal patterns and emission sources

Bo Gao[a,b], Hai Guo[b,*], Xin-Ming Wang[a,**], Xiu-Ying Zhao[a], Zhen-Hao Ling[b], Zhou Zhang[a], Teng-Yu Liu[a]

[a] State Key Laboratory of Organic Geochemistry, Guangzhou Institute of Geochemistry, Chinese Academy of Sciences, Guangzhou 510640, China
[b] Air Quality Studies, Department of Civil and Environmental Engineering, The Hong Kong Polytechnic University, Hong Kong

HIGHLIGHTS

- $PM_{2.5}$ samples were collected simultaneously at six different sites in Guangzhou.
- Tracer to PAH ratios were jointly used to identify sources of PAHs.
- Vehicular emissions were no longer the dominant PAH sources.
- More attention should be paid to coal combustion and biomass burning.

ARTICLE INFO

Article history:
Received 28 March 2012
Received in revised form 18 July 2012
Accepted 22 July 2012
Available online 24 August 2012

Keywords:
PAHs
Vehicular emissions
Coal combustion
Biomass burning
Guangzhou

ABSTRACT

Fine particulate samples were simultaneously collected at six sites in Guangzhou in November–December 2009. Eighteen polycyclic aromatic hydrocarbons (PAHs) and tracers, i.e. hopanes, elemental carbon, picene and levoglucosan were measured. Three high level episodes were observed during the sampling period, likely due to accumulation effects. Back trajectory analysis revealed that the air masses for the three episodes were from eastern inland Pearl River Delta (PRD) region. There was no obvious concentration gradient for total and 5–6 ring PAHs such as benzo[g,h,i]perylene (BghiP) from urban to rural sites. However, 4-ring PAHs such as pyrene (Pyr) exhibited significantly higher levels at rural site than that at urban/suburban sites ($p < 0.01$). BghiP correlated well with hopanes, elemental carbon and picene, indicating vehicular emissions and coal combustion were the sources of 5–6 ring PAHs, which were further confirmed by comparing the four tracers/BghiP ratios and IcdP/BghiP ratios in ambient samples with those from source profiles. Results indicated that vehicular emissions were no longer the dominant sources in winter season in Guangzhou.

1. Introduction

Polycyclic aromatic hydrocarbons (PAHs) exist widespread in the urban atmosphere and are well-known human carcinogens and mutagens. They are released mostly from incomplete combustion and pyrolysis of fossil fuels such as wood, coal and petroleum and other organic materials. PAHs associated with fine particles are of special concern because fine particles can deposit in the lungs and exert their carcinogenicity over long exposure periods. In general, PAHs with high molecular weight are mainly associated with fine particles.

Continued effort has been made worldwide to get better knowledge of PAH emissions, distributions and sources in the atmosphere [1–6]. Zhang and Tao [7] pointed out although emissions of PAHs in developed countries have decreased significantly in the past decades with the improved efficiency of energy utilization, PAH emissions from developing countries have been increasing due to rapid population growth and the associated energy demand. Xu et al. [5] estimated that the total PAH emissions in China was 25,300 tons in 2003 and the major emission sources such as biomass burning, domestic coal combustion, and coking industry contributed 60%, 20%, and 16% to the total atmospheric PAH emission, respectively.

The major sources of PAHs in Guangzhou are vehicular emission, biomass burning and coal combustion [8–10]. Early studies performed in 2001 identified vehicular emissions as the dominant sources of PAHs in urban Guangzhou [8,9]. A recent research reported that in winter, regional biomass burning could be the

* Corresponding author at: Department of Civil and Environmental Engineering, Hong Kong Polytechnic University, Hong Kong. Tel.: +852 3400 3962; fax: +852 2334 6389.
** Corresponding author at: Guangzhou Institute of Geochemistry, Chinese Academy of Sciences, China. Tel.: +86 20 85290180; fax: +86 20 85290706.
E-mail addresses: ceguohai@polyu.edu.hk (H. Guo), wangxm@gig.ac.cn (X.-M. Wang).

0304-3894/$ – see front matter © 2012 Elsevier B.V. All rights reserved.
http://dx.doi.org/10.1016/j.jhazmat.2012.07.068

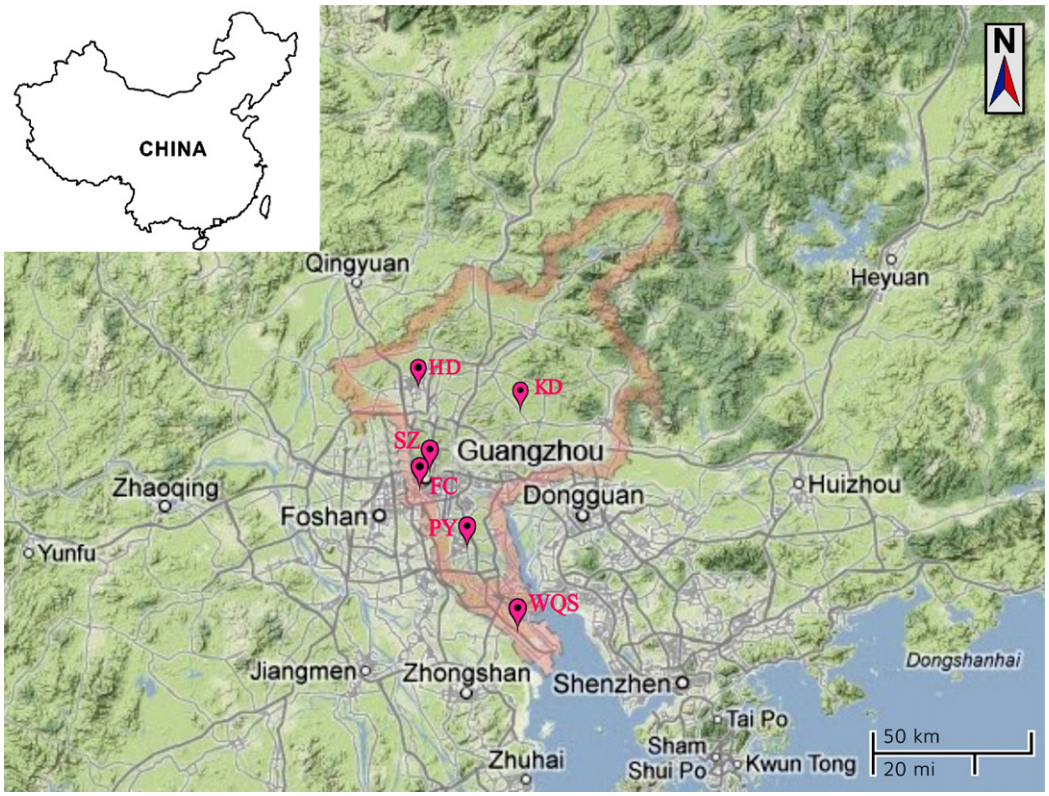

Fig. 1. Location of the six sampling sites.

dominant sources of high molecular PAHs such as IcdP and BghiP in Guangzhou [10]. However, as these studies were conducted at only one or two sites, they cannot provide a full picture of PAHs in Guangzhou. In addition, the source identification methods adopted in these studies were mainly PAH ratios and principle component analysis using only PAH data. These methods have been challenged by the degradation of certain PAHs, overlapped ratios and similar PAH profiles among different sources. As it has been years since previous source identifications in Guangzhou were carried out, the dominant PAH sources may be significantly changed due to the fact that energy generation and consumption have been greatly restructured and increased, and strict vehicular emission standards have been taken effect and numerous high emission vehicles have been phased out in the past decade in Guangzhou. Therefore, it is necessary to reevaluate the sources of PAHs in Guangzhou using more reliable methods.

Pearl River Delta (PRD) region is a highly industrialized and densely populated city cluster. Studies have shown that cities in this region suffer from regional air pollution [11–13]. As one class of persistent organic pollutants, PAHs can undergo long range atmospheric transport. PAHs emitted from a location can be deposited to remote receptors. Guangzhou, with an area of 7434 km^2, is the economic and cultural center of the PRD. During the past decade, the population in Guangzhou increased from 6.9 million in 2000 to 10.3 million in 2009. More and more people have the potential to be exposed to PAH-associated polluted air. Therefore, it is important to know the source regions and pathways, and the regional impact on airborne PAHs in the atmosphere of Guangzhou.

This study benefits from the intensive sampling campaigns at six different sites in Guangzhou from 28 November to 23 December 2009. $PM_{2.5}$ samples were collected and measured for major components and various organic compounds. 18 PAHs together with certain molecular tracers for vehicular emissions (i.e. hopanes and elemental carbon), coal combustion (i.e. picene) and biomass burning (i.e. levoglucosan) in the samples were analyzed. With this large dataset, better understanding of the spatiotemporal variations of PAH levels can be achieved. By means of back trajectory cluster analysis, the air mass source regions and pathways, and the regional influence on PAHs are discussed. Finally, the sources of PAHs are evaluated by their correlations with tracers and by comparison of the percentages of several tracers to PAH ratios in the samples with those calculated from multiple source profiles.

2. Materials and methods

2.1. Sampling sites

Six sites were selected for the field measurements including Guangzhou Environmental Monitoring Center (SZ) and Guangdong Fangcun Experimental High School (FC) in urban areas, Huadu Normal College (HD) and Pan Yu Middle School (PY) in suburban areas, and Guangzhou Kangda Vocational Technical College (KD) and Wanqingsha middle school (WQS) in rural areas (Fig. 1). The distances between every two sites with the same land-use function were approximately 7, 55 and 65 km for urban, suburban and rural areas, respectively.

SZ (23.13°N, 113.27°E) and FC (23.07°N, 113.23°E) were in the city center, with heavy traffic and busy commercial activities. HD (23.39°N, 113.22°E) was located in a newly-developed industrial area with light traffic, about 30 km north from Guangzhou city center and 9 km west from the Baiyun international airport. PY (22.94°N, 113.36°E) was about 25 km southeast from the city center. It was located in a newly-developed residential town with scattered houses, schools and light traffic but adjacent to the highway and to railway lines. KD (23.30°N, 113.57°E), about 40 km northeast from urban center, was located in a mountainous and hilly area with sparse population. There was a main road with rare traffic approximately 200 m away from this site. The

southernmost site WQS (22.71°N, 113.55°E) was located in a small town in the central PRD, surrounded by city clusters (e.g. Hong Kong, Guangzhou, Shenzhen, Foshan and Dongguan), about 55 km away from city center and adjacent to the Pearl River estuary. This small town was surrounded by farmlands and had very few textile and clothing workshops. However, this town was adjacent to a busy highway.

2.2. Fine particle sampling

At each site, a high volume sampler (Tisch Environmental, Inc.) was deployed to collect $PM_{2.5}$ samples at a constant flow rate of 1.1 $m^3\ min^{-1}$ at the rooftop of a seven-storey building with a height of 30 m above the ground. 24-h samples (10 a.m.–10 a.m.) were taken consecutively from 28 November to 23 December 2009. Samples at all sites were not collected on 8 and 9 December because of raining. Due to logistical difficulty, samples on 3 and 15 December at SZ, on 6 December at PY, on 10 and 16 December at KD and on 10, 15 and 16 December at WQS were not taken. In total, 136 samples were collected on quartz filters (Whatman, Mainstone, UK). 8 × 10 in. filters were pre-heated for 12 h at 450 °C and stored at 4 °C wrapped with aluminum foil before collection and at −20 °C after collection.

2.3. Chemical analysis

A punch (1.5 cm × 1.0 cm) of each filter was taken for the measurements of organic carbon (OC) and elemental carbon (EC) using the thermo-optical transmittance (TOT) method by an OC/EC Analyzer (Sunset Laboratory Inc.) Detailed analytical procedures are described in NIOSH [14].

For the analysis of PAHs, hopanes and levoglucosan, detailed description is given elsewhere [10]. Briefly, a mixture of three isotopically labeled PAH compounds (phenanthrene-d10, chrysene-d12, and perylene-d12), tetracosane-d50 and levoglucosan-$^{13}C_6$ were added as surrogates prior to extraction. $PM_{2.5}$ filter samples were ultrasonically extracted twice with 40 mL hexane, then three times with 40 mL dichloromethane (DCM)/methanol (1:1, v/v). The extracts were concentrated to 1 mL and split into two aliquots. One aliquot (~0.5 mL) was solvent-exchanged to redistilled hexane, and then purified using a 1:2 alumina/silica column chromatography. Two fractions were eluted. The first fraction containing nonpolar compounds was eluted by 30 mL of hexane. The second fraction was eluted by 70 mL of DCM/hexane (3:7, v/v). The two fractions were combined, concentrated to ~2 mL and blown to dryness under a gentle stream of nitrogen. This was redissolved with n-hexane to ~0.5 mL and analyzed for PAHs (including picene) and hopanes. The other aliquot (~0.5 mL) was blown to dryness for silylation with 100 μL of pyridine and 200 μL of BSTFA (BSTFA/TMCS, 99:1, Supelco) in an oven at 70 °C for 1 h. The silylated extract was then analyzed for levoglucosan.

The samples were analyzed using an Agilent GC–MS (6890-5973N) equipped with a DB-5MS column (50 m × 0.32 mm × 0.17 μm). The column temperature was initiated at 80 °C (held for 2 min) and increased to 290 °C at 4 °C min^{-1} (held for 30 min). An aliquot of 1 μL was injected in splitless/split mode with a solvent delay of 6 min. Target compounds were identified based on their mass spectra and retention times. Molecular ions, m/z 191 and m/z 60 were used as target ions for the quantification of PAHs, hopanes and levoglucosan, respectively.

In this study, PAH compounds analyzed are given as follows: naphthalene (Nap), acenaphthylene (Acey), acenaphthene (Ace), fluorene (Fl), phenanthrene (Phe), anthracene (Ant), fluoranthene (Flu), pyrene (Pyr), benz[a]anthracene (BaA), chrysene (Chr), benzo[b]fluoranthene (BbF), benzo[k]fluoranthene (BkF), benzo[e]pyrene (BeP), benzo[a]pyrene (BaP), indeno[1,2,3-cd]pyrene (IcdP), benzo[g,h,i]perylene (BghiP), dibenz[a,h]anthracene (DahA) and Coronene (Cor).

Field blanks and lab blanks were routinely analyzed to determine any background contamination. All results showed very low analytes and in most cases not detectable in the blanks. Recovery efficiencies were determined by evaluating surrogate recovery standards spiked to the samples. The mean recoveries for surrogates in field samples were naphthalene-d8 30%, acenaphthalene-d8 33%, phenanthrene-d10 35%, chrysene-d12 88%, perylene-d12 70%, tetracosane-d50 90% and levoglucosan-$^{13}C_6$ 88%. It is noteworthy that the recovery of naphthalene-d8, acenaphthalene-d8 and phenanthrene-d10 was relatively low due to their high volatility. Since 2–3 ring PAHs mainly exist in gas phase, they are not the focus in this study.

2.4. Selection of molecular tracers

In contrast to PAHs having various sources, molecular tracers are more source-specific and have been widely used to identify sources [4,15–18]. As previous studies identified that the main sources of PAHs in Guangzhou were vehicular emissions (VE), biomass burning (BB) and coal combustion (CC) [8–10], tracers for these sources were selected: hopanes and EC as tracers of VE [4,17], levoglucosan as a tracer of BB [4,16] and picene as a tracer of CC [19,20]. In this study, different hopane compounds were highly correlated with each other ($R^2 > 0.85$). The levels of four dominant hopanes, i.e. 17α(H)-21β(H)-29-Norhopane, 17α(H)-21β(H)-Hopane, 22S-Homohopane and 22R-Homohopane, were summed up (denoted as $\sum_4$Hopanes) to represent total hopanes.

3. Results and discussion

3.1. Meteorological conditions

The meteorological data of Guangzhou during the sampling period were obtained from a website (http://www.tqjlw.cn), which provided weather data of major cities in China. The daily variations of ambient temperature, relative humidity, wind speed and wind direction during the sampling period are shown in Fig. 2a. The daily temperature was 10.8–22.6 °C with an average of 16.0 °C. The daily relative humidity was 34.2–94.0% with an average of 65.1%. The daily wind speed was 3.6–20.0 km h^{-1} with an average of 9.8 km h^{-1}. The dominant wind directions were from the north and northeast. There was a precipitation from 6 p.m. on 7 December to 9 a.m. on 8 December, and no rain on the other sampling days.

3.2. Temporal variation of PAHs

Correlation analysis on the concentrations of individual PAHs for all the sampling sites revealed that three groups of PAHs had strong correlations ($R^2 > 0.85$), namely (1) Flu and Pyr; (2) BaA and Chr; and (3) 5–7 ring PAHs. This indicated that PAHs with comparative ring sizes had similar physiochemical properties and/or emission sources. Hence, three typical PAHs, i.e. Pyr, Chr and BghiP were selected to represent each corresponding group in this study. Fig. 2b shows the temporal variations of the three PAHs. The OC, EC and molecular tracers are also shown in Fig. 2b for the comparison of the temporal trends of these species.

It was found that all species including sum of all species at all sites had similar temporal variations and they exhibited three high-value episodes, i.e. 4–6 (H1), 10–12 (H2) and 21–23 (H3) December and two low-value episodes, i.e. 29 November–3 December (L1) and 15–20 (L2) December. The PAH concentrations during high episodes were significantly higher than those during low episodes ($p < 0.01$). For example, BghiP averaged 1.29 ± 0.14, 3.66 ± 0.87,

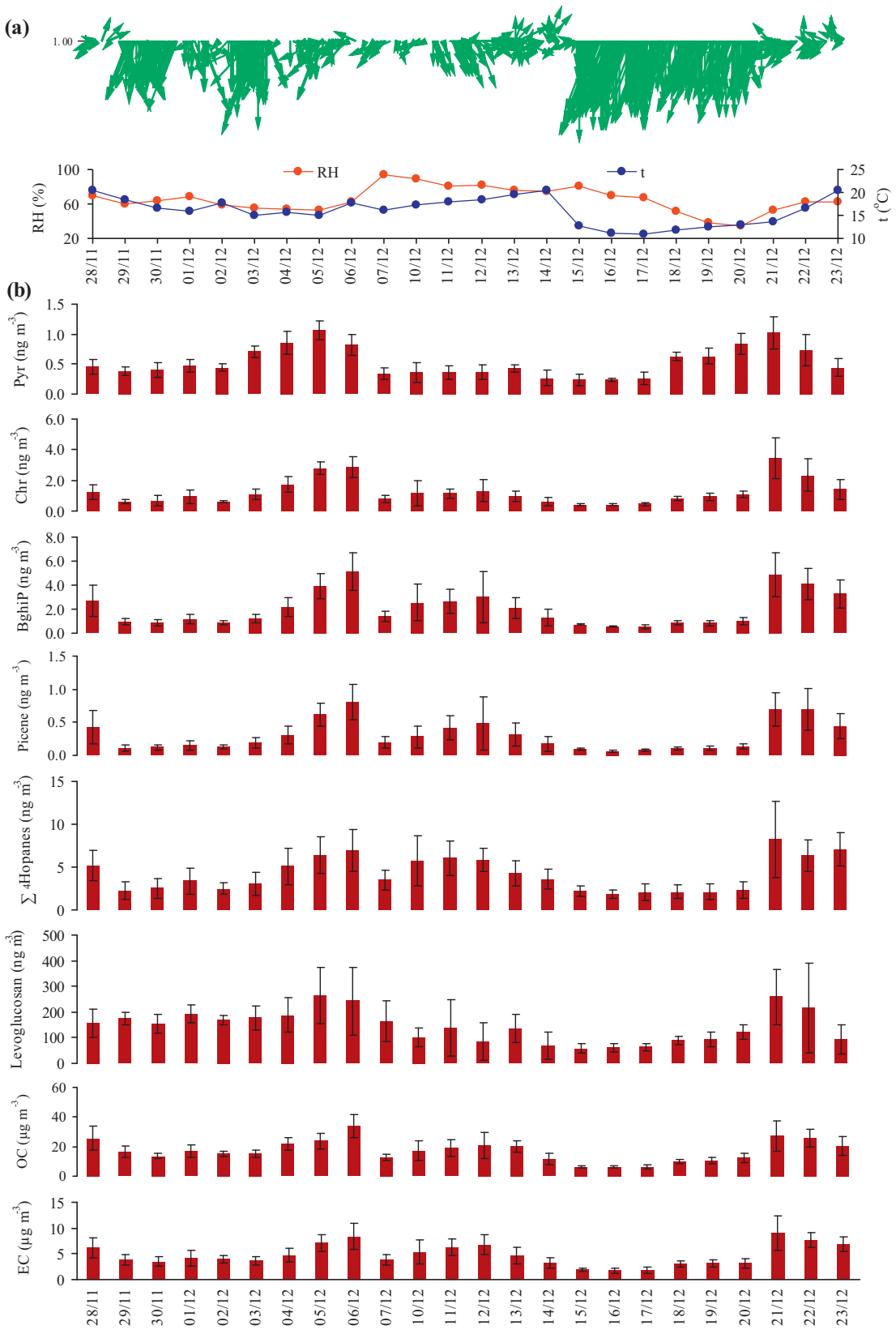

Fig. 2. Daily variations of (a) ambient temperature, relative humidity, wind speed and wind direction for Guangzhou city; (b) PAHs, Σ_4Hopanes, levoglucosan, OC and EC at the six sampling sites in Guangzhou from 28 November to 23 December 2009.

Table 1
PAH concentrations (ng m^{-3}) at the six sampling sites.

	SZ (n = 22)		FC (n = 24)		PY (n = 23)		HD (n = 24)		KD (n = 22)		WQS (n = 21)	
	Mean (95%CI) [a]	Median	Mean (95%CI) [a]	Median	Mean (95%CI) [a]	Median	Mean (95%CI) [a]	Median	Mean (95%CI) [a]	Median	Mean (95%CI) [a]	Median
Nap	0.04 (0.02)	0.04	0.05 (0.02)	0.04	0.03 (0.01)	0.02	0.04 (0.02)	0.04	0.03 (0.01)	0.03	0.02 (0.01)	0.02
Acey	0.02 (0.01)	0.01	0.04 (0.01)	0.04	0.01 (0.01)	0.01	0.03 (0.01)	0.03	0.01 (0.01)	0.01	0.01 (0.01)	0.01
Ace	0.02 (0.01)	0.01	0.04 (0.01)	0.04	0.01 (0.00)	0.01	0.03 (0.01)	0.03	0.01 (0.01)	0.01	0.01 (0.00)	0.01
Fl	0.04 (0.02)	0.03	0.06 (0.02)	0.05	0.02 (0.01)	0.02	0.04 (0.02)	0.04	0.02 (0.01)	0.02	0.03 (0.01)	0.03
Phe	0.15 (0.03)	0.14	0.19 (0.04)	0.17	0.13 (0.03)	0.11	0.17 (0.03)	0.16	0.15 (0.03)	0.14	0.12 (0.03)	0.09
Ant	0.08 (0.01)	0.07	0.10 (0.02)	0.09	0.06 (0.01)	0.06	0.08 (0.02)	0.07	0.07 (0.01)	0.06	0.07 (0.01)	0.06
Flu	0.47 (0.09)	0.42	0.64 (0.15)	0.55	0.45 (0.12)	0.37	0.64 (0.12)	0.52	0.69 (0.13)	0.61	0.73 (0.16)	0.62
Pyr	0.43 (0.07)	0.39	0.58 (0.13)	0.50	0.40 (0.10)	0.35	0.56 (0.11)	0.48	0.65 (0.13)	0.60	0.63 (0.13)	0.57
BaA	0.71 (0.23)	0.51	1.12 (0.45)	0.71	0.54 (0.25)	0.36	0.96 (0.35)	0.53	0.88 (0.27)	0.65	0.46 (0.11)	0.38
Chr	1.11 (0.31)	0.84	1.70 (0.54)	1.30	0.88 (0.35)	0.61	1.40 (0.47)	0.87	1.25 (0.35)	0.91	1.17 (0.24)	1.07
BbF	1.99 (0.52)	1.51	3.00 (0.90)	2.24	1.62 (0.57)	1.12	2.70 (0.85)	1.72	2.24 (0.64)	1.46	2.08 (0.49)	1.56
BkF	1.38 (0.36)	1.09	2.12 (0.65)	1.57	1.20 (0.47)	0.81	1.98 (0.67)	1.18	1.60 (0.48)	1.04	1.69 (0.35)	1.41
BeP	1.81 (0.44)	1.41	2.72 (0.77)	2.09	1.56 (0.56)	1.08	2.46 (0.78)	1.54	1.97 (0.56)	1.30	1.82 (0.37)	1.64
BaP	1.16 (0.39)	0.87	1.67 (0.60)	1.23	1.11 (0.47)	0.71	1.70 (0.63)	1.01	1.47 (0.51)	0.76	1.14 (0.31)	0.89
IcdP	3.12 (0.87)	2.59	4.05 (1.33)	2.96	2.48 (1.14)	1.39	4.54 (1.60)	2.87	3.22 (1.07)	1.75	2.26 (0.54)	1.91
DahA	0.37 (0.12)	0.30	0.52 (0.17)	0.35	0.28 (0.13)	0.15	0.55 (0.21)	0.33	0.39 (0.13)	0.25	0.21 (0.07)	0.18
Picene[b]	0.26 (0.07)	0.20	0.36 (0.12)	0.26	0.20 (0.11)	0.10	0.43 (0.17)	0.30	0.31 (0.11)	0.18	0.21 (0.06)	0.15
BghiP	1.94 (0.52)	1.64	2.45 (0.79)	1.76	1.62 (0.72)	0.93	2.71 (0.94)	1.69	1.88 (0.61)	1.05	1.59 (0.38)	1.27
Cor	0.64 (0.19)	0.58	0.62 (0.20)	0.47	0.54 (0.28)	0.21	0.90 (0.33)	0.48	0.51 (0.17)	0.31	0.54 (0.14)	0.40
ΣPAHs	15.46 (4.25)	11.97	21.65 (6.52)	15.35	12.94 (4.99)	8.06	21.46 (6.92)	12.97	17.02 (5.23)	11.31	14.46 (3.25)	12.83
Σ_4Hopanes[c]	5.38 (1.22)	4.57	6.40 (1.44)	5.34	3.46 (0.74)	2.53	3.38 (1.02)	2.38	2.26 (0.58)	1.67	4.38 (0.53)	4.71
Levoglucosan	118.40 (20.66)	122.47	131.17 (38.74)	120.29	89.70 (17.99)	82.11	179.04 (40.17)	177.08	251.75 (55.00)	220.18	109.99 (24.31)	120.23
OC ($\mu g\,m^{-3}$)	17.81 (3.64)	15.47	22.61 (4.30)	21.55	13.62 (2.47)	12.64	18.27 (4.03)	15.41	15.12 (3.27)	14.31	15.70 (2.31)	16.27
EC ($\mu g\,m^{-3}$)	5.58 (1.13)	4.91	6.32 (1.32)	5.12	3.78 (0.81)	3.24	4.18 (0.99)	3.27	4.03 (1.03)	2.95	4.94 (0.63)	5.08

[a] Numbers in parentheses are the 95% confidence interval.

[b] Not included in ΣPAHs.

[c] The four hopanes are 17α(H)-21β(H)-29-Norhopane, 17α(H)-21β(H)-Hopane, 22S-Homohopane and 22R-Homohopane.

Table 2
Correlation coefficients (R^2) of Pyr, Chr and BghiP among the six sampling sites.

Pyr, Chr, BghiP	SZ	FC	PY	HD	KD	WQS
SZ	1, 1, 1					
FC	0.50, 0.60, 0.64	1, 1, 1				
PY	0.78, 0.70, 0.54	0.52, 0.80, 0.52	1, 1, 1			
HD	0.69, 0.50, 0.53	0.45, 0.42, 0.39	0.61, 0.36, 0.27	1, 1, 1		
KD	0.64, 0.69, 0.67	0.51, 0.62, 0.55	0.45, 0.44, 0.30	0.85, 0.84, 0.77	1, 1, 1	
WQS	0.53, 0.22, 0.155	0.57, 0.31, 0.23	0.77, 0.37, 0.38	0.29, 0.03, 0.03	0.24, 0.06, 0.01	1, 1, 1

2.76 ± 0.94, 0.77 ± 0.10 and 4.07 ± 0.86 ng m^{-3} for L1, H1, H2, L2 and H3, respectively. It is well known that the concentrations of air pollutants have close relationships with meteorological conditions. During the three high-value episodes, the weather conditions were stable, namely relatively high temperature and solar radiation, and low wind speeds, which were favorable for the accumulation of PAHs. On the other hand, during the two low-value episodes, there were two cooling processes caused by cold front and/or rain belts, which lowered the PAH concentrations. For instance, from 14 to 15 December, the temperature fell sharply from 20.4 to 12.8 °C and the prevailing northerly wind accelerated from a speed of 5.3 to 19.0 km h^{-1}, leading to strong mixing and dispersion of air and subsequently the reduction of all species to significantly low levels ($p < 0.01$). Indeed, the mean BghiP level was 1.55 ± 0.71 ng/m^3 on 14 December and 0.73 ± 0.07 ng/m^3 on 15 December. It is noteworthy that on 7 December, after several days' accumulation of PAHs, there was a sharp decrease in PAH levels, most likely due to the washout effect by the rain from 6 p.m. on 7 December to 9 a.m. on 8 December.

In addition, by averaging all the samples collected at the six sites, the average profile of PAHs in the atmosphere of Guangzhou was obtained (Fig. S1). Clearly, IcdP had the highest concentration, followed by BbF, BghiP and BeP. Inversely, the concentrations of NaP, Acey, Ace, Fl and Ant in the atmosphere of Guangzhou were negligible.

3.3. Spatial variation of PAHs

The mean concentrations together with 95% confidence intervals of individual PAHs at the six sampling sites in Guangzhou are given in Table 1. The total PAH concentrations ranged from 2.67 to 68.9 ng m^{-3}, with an average value of 17.1 ng m^{-3}. The dominant species were 5–7 ring PAHs, accounting for ~80% of the total PAHs. By comparison, the total PAH concentrations found in this study are consistent with those reported by Li et al. [9] and Yang et al. [21], who found that the total PAH concentrations were 10–40 ng m^{-3} in December 2001 in Guangzhou, and ranged from 29.7 to 39.1 ng m^{-3} in December 2005, respectively. Bearing the large variations in mind, the total PAH concentrations were the highest at FC and HD, and the lowest at PY. Inspection found that all the tracers showed slightly higher levels at urban FC than those at urban SZ, indicating that the air was more polluted at FC due to stronger source emissions. Relatively high PAH concentrations at HD may be explained by more BB and CC, as indicated by relatively high levogulcosan and

Fig. 3. Back trajectory cluster analysis during the sampling period.

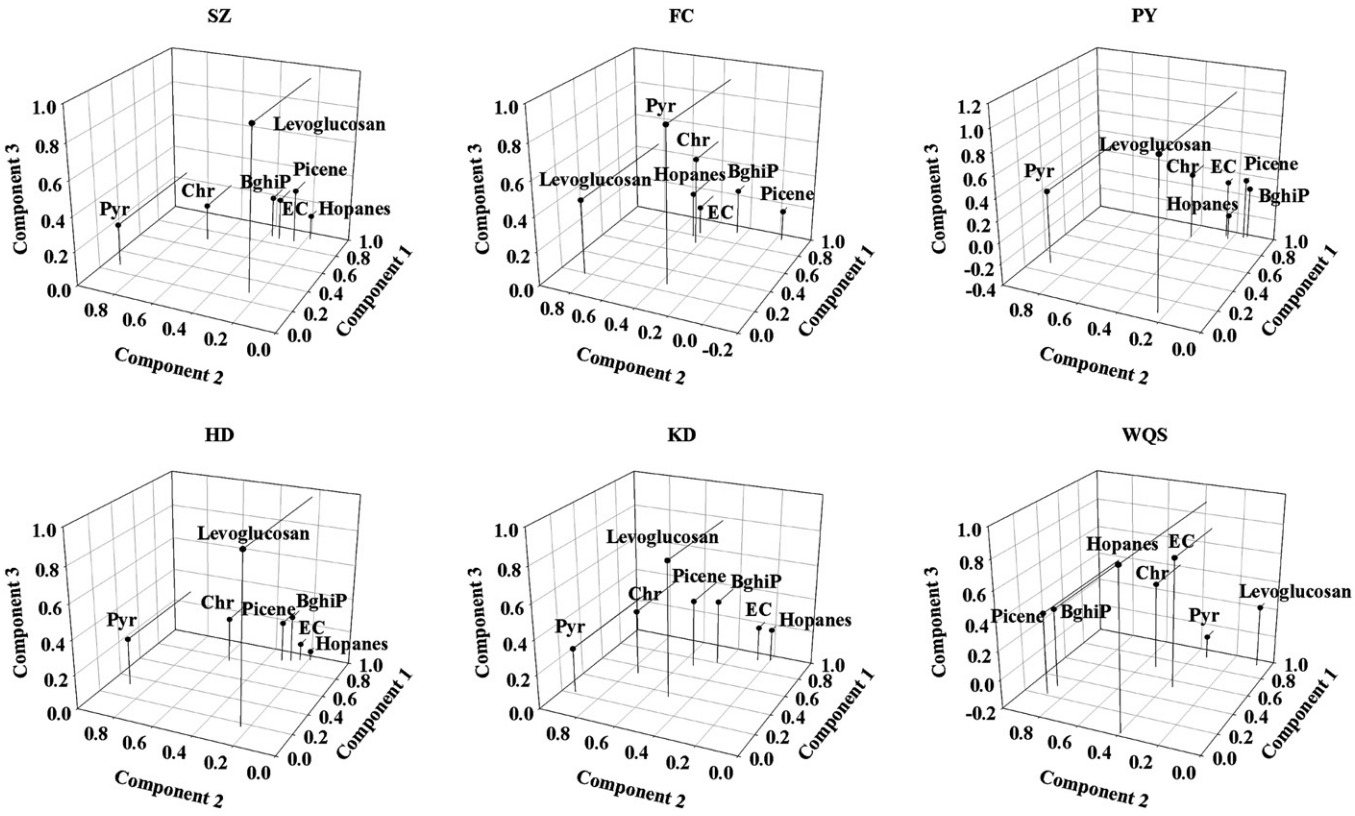

Fig. 4. Principal component analysis factor loading plot.

picene levels. Indeed, MODIS fire maps showed many open fires in the northern direction of HD during the sampling period (Fig. S2). As the coal-fired industry was mainly populated in the urban center, the relatively high CC emissions at HD could be more related to small and low-efficient coal-fired boilers and domestic CC. Slightly higher PAH levels at KD and WQS than those at PY may be due to more BB emissions at the two rural sites, where the residents traditionally burned straws, stalks and deadwood for cooking and heating. In addition, KD was also influenced by the northern upwind BB emissions from open fires (Fig. S2).

Similar to the total PAHs, 5–7 ring PAH levels did not show significant difference among the sites. 4-ring PAHs such as Pyr and Chr, however, exhibited some spatial patterns. The mean Pyr level at KD was significantly greater than that at SZ and PY ($p < 0.01$) while the mean Chr level at FC was much higher than that in PY ($p < 0.05$). The different spatial patterns of the three PAHs among the sites may be due to the difference in factors such as source emission strengths, micro-environmental meteorological conditions and atmospheric transportations.

It is well known that BaP is the most carcinogenic PAH among the 16 USEPA PAHs. It has often been used as an indicator of the carcinogenicity of PAHs. The mean levels of BaP were 1.16 ± 0.39, 1.67 ± 0.60, 1.11 ± 0.47, 1.70 ± 0.63, 1.47 ± 0.51, and 1.14 ± 0.31 ng m^{-3} at SZ, FC, PY, HD, KD and WQS, respectively. In addition to BaP, other species such as BaA, BbF, BkF, DahA and IcdP are usually considered as possible human carcinogens [22–24]. Exposure to these carcinogenic compounds may cause respiratory, cardiovascular and other long-term chronic diseases [25]. To assess the carcinogenic potency of PAHs, the cancer potency equivalence factors (BaP_{eq}) of target carcinogenic PAHs were calculated using the following equation:

$$BaP_{eq} = BaA \times 0.06 + BF \times 0.07 + BaP + DahA \times 0.6 + IcdP \times 0.08$$

The cancer potency equivalency factors (PEF) proposed by Yassaa et al. [26] were used. Hence, the BaP_{eq} was 1.91 ± 0.60, 2.73 ± 0.94, 1.71 ± 0.72, 2.78 ± 1.00, 2.28 ± 0.77 and 1.74 ± 0.44 ng m^{-3} at SZ, FC, PY, HD, KD and WQS, respectively. The average BaP_{eq} values at all sites exceeded 1 ng m^{-3}, namely the WHO air quality guideline recommended for BaP as daily average, indicating the health risk of exposure to these carcinogenic PAHs in Guangzhou.

3.4. Impact of inland and outland PRD

As one class of persistent organic pollutants, PAHs have relatively long lifetimes in the atmosphere and can travel long distance from one location to other places. In order to find the relationships of PAH levels among different sites, correlation analysis of the three typical PAHs between every two sites was carried out. It can be seen that for all the three PAHs, most of the site–site correlations were moderate–good (Table 2, $R^2 = 0.39$–0.78), indicating the prevalence of regional influence over Guangzhou. In particular, the highest correlations between KD and HD were found for the three PAHs, perhaps due to the significant influence of the northern upwind BB emissions from open fires (Fig. S2). In contrast, the PAHs at WQS showed the lowest correlations with those at other sites, especially for Chr and BghiP, indicating that the emission sources and/or emission patterns of these PAHs at WQS may be different from those at the other sites.

To understand the pathways of air masses and the percentage of each class of air masses, back trajectory cluster analysis was carried out. Air mass backward trajectories were calculated using NOAA-HYSPLIT (v4.9) model. The meteorological data that drove the model were from the Global Data Assimilation System (GDAS) data set (3 hourly, global, 1° in longitude and latitude, and 23 pressure levels). For each sampling day, 10-h backward

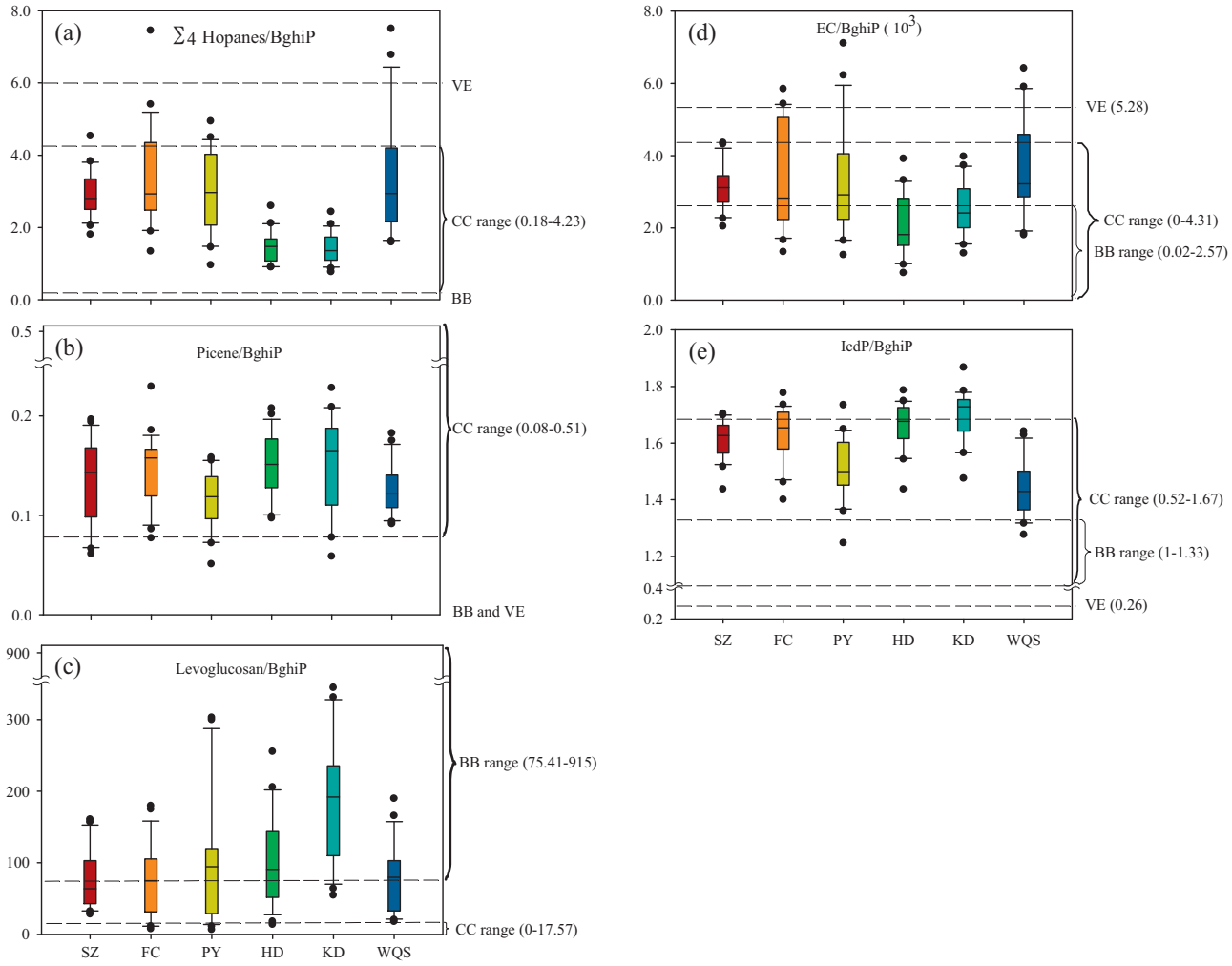

Fig. 5. Σ_4Hopanes/BghiP (a), picene/BghiP (b), levoglucosan/BghiP (c), EC/BghiP (d) and IcdP/BghiP (e) ratios for the six sites. The vehicular emission composition is from data collected in Zhujiang Tunnel in the western urban area of Guangzhou [30]. The biomass burning profiles are obtained from rice straw and sugar cane burning in open field burning in the PRD [31] and several biomass burning in dilution chamber measurements [32]. The coal combustion profiles are selected from coal combustion in the main coal-mining regions in China [19].

trajectories starting at 0:00, 6:00, 12:00 and 18:00 with the ending point of 200 m above sea level were configured. Finally, during the 24-day sampling period, 96 back trajectories were obtained in total. The trajectories were combined successively to form different groups by increasing the cluster total spatial variance (TSV). In this study, the final group number was determined by the percent change in TSV and grouping performance. Two clusters are classified as shown in Fig. 3. The first cluster originated from the east border of inland PRD, i.e. Huizhou (track 1), accounting for 59% of the total air masses. The second cluster (track 2) originated from northern outland PRD, near the boundary of Guangdong and Jiangxi provinces, contributing 41% to the total air masses. This track passed over Shaoguan and Conghua, and travelled much faster than the first track. The endpoints associated with track 2 were mostly labeled on 29 November, 2–3, and 15–20 December. Further inspection found that the wind speeds on these days (12.53–19.95 km h^{-1}) were higher than those on the other days (3.60–10.47 km h^{-1}). As discussed in Section 3.2, on days associated with track 2, the cooling process happened and PAH levels were significantly lower than those on the other days ($p < 0.01$). It is noteworthy that track 1 included the three high level episodes while track 2 stood for air masses on days when strong Asian winter monsoon was dominant, which brought cold and clean air and sharply reduced pollutant levels at the sites. As expected, under the influence of the two different air masses, the pollutant levels at the sites exhibited large variations (Fig. 2).

3.5. Source identification

To obtain initial information on the relationships between individual PAHs and the tracers, principal component analysis factor loading plots of three PAHs together with tracers for the six sites are presented in Fig. 4. For each site, three components with cumulative variance explained larger than 95% were extracted based on the main sources in Guangzhou as mentioned above. It is interesting to note that from BghiP to Pyr, with the decrease of molecular weight, their relations with picene, $\sum_4$Hopanes and EC weakened but this trend was not apparent for levoglucosan. This might be caused by the larger influence of the gas-particle partitioning on the 4-ring PAHs than on 5–6 ring PAHs. The effect of gas-particle partitioning might bias the source identification for 4-ring PAHs. In addition, 5–6 ring PAHs predominantly exist in particle phase and are major PAHs that induce health effect. Therefore, we mainly focused on 5–6 ring PAHs such as BghiP for their source identification.

Excellent associations were found between BghiP and picene for all the six sites, indicating that CC had significant influence on this PAH. Moderate to good associations of BghiP with $\sum_4$Hopanes and EC suggested the strong impact of VE on BghiP levels. The relatively weaker associations between BghiP and levoglucosan compared to other tracers may be due to the strong variations of levoglucosan. Compared to CC and VE, BB was characterized by more irregular emissions and thus larger day-to-day variations. In addition, combustion materials and conditions also had significant impact on the emissions of levoglucosan.

Although PAH ratios have been widely used to distinguish the sources of PAHs, the degradation of individual compounds will potentially undermine the application of the ratios as a reliable source identification tool [27]. Moreover, different sources often have similar or overlapped PAHs ratios, which result in the difficulty in identifying the major sources. Instead, the use of specific tracers other than PAHs becomes fundamental for the identification of these sources [4]. We believe different source categories have distinct tracers to PAH ratios. Fig. 5 shows the percentiles of several tracers to BghiP ratios. As single ratio may not provide reliable identification of major sources, four tracers to BghiP ratios, i.e. Σ_4Hopanes/BghiP, picene/BghiP, levoglucosan/BghiP and EC/BghiP, and one commonly used PAH ratio, i.e. IcdP to BghiP, were jointly used. IcdP to BghiP ratio was selected because the two PAHs are photolytically degraded at comparable rates and therefore their ratios retain the characteristics of emission sources [28,29]. Also plotted in Fig. 5 are ratio ranges obtained from source profiles measured in other studies [19,30–32]. It is practical to select source profiles that could represent local emissions. In this study, The VE profile was from data collected in Zhujiang Tunnel in Guangzhou [30]. Because of large variations of CC emission factors [5,33] and high uncertainties in BB emissions [34] in PRD, more profiles were selected for these two sources. The BB profiles were obtained from rice straw and sugar cane burning in open field burning in the PRD [31], and from the BB measured in dilution chamber in South Asia [32]. The CC profiles were selected from CC in the main coal-mining regions in China [19]. In total, seven BB profiles and eight CC profiles were selected.

It can be seen that for all the six sites, most ratios of ambient data were quite away from the ratios of VE source profile, indicating VE was not the dominant source of BghiP (Fig. 5). Nevertheless, although most ratios (>50%) fell into the CC range (Fig. 5), it could not be inferred that CC emissions were the dominant sources of BghiP, because the range of CC was very wide and the ratios could be explained by random combinations of VE, BB and CC. The Σ_4Hopanes/BghiP and EC/BghiP ratios at KD were significantly lower than those at SZ, FC, PY and WQS (Fig. 5b and d), whereas the levoglucosan/BghiP ratios showed higher values at KD (Fig. 5c), suggesting that BB rather than VE was the main source of BghiP at KD, in line with the fact that this site was located in a rural area.

Previous studies in Guangzhou claimed VE as the dominant source of PAHs, especially for BghiP and IcdP [8,9], in contrast to the findings in this study. The shift of source contributions may be due to strict VE control over years [35], but rare control for CC and BB in PRD. However, the notion that VE was no longer the dominant source of PAHs should be examined by source apportionment tool such as positive matrix factorization (PMF). Moreover, as we only studied one month data in winter Guangzhou, future research is needed to update our knowledge about the seasonal and annual variations of source contributions to PAHs in Guangzhou.

4. Summary

24-h $PM_{2.5}$ samples were collected simultaneously at six sites in Guangzhou from 28 November to 23 December. The total PAH concentrations measured were from 2.66 to 68.51 ng m^{-3}, with an average value of 17.13 ng m^{-3}. Individual PAHs and major components such as organic and elemental carbon exhibited similar temporal patterns. There were two high-PAH episodes on 4–6 and 21–23 December due to the accumulation under the influence of stable boundary layer, elevated temperature and low wind speeds when the cooling processes were over. There were no significant differences of the total and 5–6 ring PAHs among the sites. 4-ring PAHs such as Pyr and Chr, however, exhibited some spatial variations, implying the differences in source emission strengths, micro-environmental meteorological conditions and atmospheric transportations among the sites. Back trajectory cluster analyses showed that the air masses arrived in Guangzhou had different origins, i.e. the east border of inland PRD and the northern outland PRD. While the 6-ring PAH species BghiP correlated well with molecular tracers such as hopanes, EC and picene, 4-ring PAH species Pyr and Chr showed poor–moderate correlations with these tracers, perhaps due to the influence of gas-particle partitioning on the 4-ring PAHs. In order to identify the sources of 5–6 ring PAHs, tracer/BghiP and IcdP/BghiP ratios were used. The results indicated that vehicular emissions were not the dominant sources of BghiP in winter Guangzhou. However, further study is necessary to update our knowledge about seasonal and annual patterns of PAH source apportionment in Guangzhou.

Acknowledgements

This study is supported by the National Natural Science Foundation of China (project no. 40821003/41025012), the Research Grants Council of the Hong Kong Special Administrative Region (project no. PolyU 5179/09E), and the Joint Scheme of National Natural Science Foundation of China and Research Grants Council of Hong Kong (NSFC/RGC joint project no. N_PolyU545/09). This project is partially supported by the Hong Kong Polytechnic University Internal Fund (project no. 1-ZV7A).

Appendix A. Supplementary data

Supplementary data associated with this article can be found, in the online version, at http://dx.doi.org/10.1016/j.jhazmat.2012.07.068.

References

[1] R.M. Harrison, D.J.T. Smith, L. Luhana, Source apportionment of atmospheric polycyclic aromatic hydrocarbons collected from an urban location in Birmingham, UK, Environ. Sci. Technol. 30 (1996) 825–832.
[2] H. Guo, S.C. Lee, K.F. Ho, X.M. Wang, S.C. Zou, Particle-associated polycyclic aromatic hydrocarbons in urban air of Hong Kong, Atmos. Environ. 37 (2003) 5307–5317.
[3] R.K. Larsen, J.E. Baker, Source apportionment of polycyclic aromatic hydrocarbons in the urban atmosphere: a comparison of three methods, Environ. Sci. Technol. 37 (2003) 1873–1881.
[4] B.L. van Drooge, P.P. Ballesta, Seasonal and daily source apportionment of polycyclic aromatic hydrocarbon concentrations in PM10 in a semirural European area, Environ. Sci. Technol. 43 (2009) 7310–7316.
[5] S.S. Xu, W.X. Liu, S. Tao, Emission of polycyclic aromatic hydrocarbons in China, Environ. Sci. Technol. 40 (2006) 702–708.
[6] Y.X. Zhang, S. Tao, J. Cao, R.M. Coveney, Emission of polycyclic aromatic hydrocarbons in China by county, Environ. Sci. Technol. 41 (2007) 683–687.
[7] Y.X. Zhang, S. Tao, Global atmospheric emission inventory of polycyclic aromatic hydrocarbons (PAHs) for 2004, Atmos. Environ. 43 (2009) 812–819.
[8] X.H. Bi, G.Y. Sheng, P. Peng, Y.J. Chen, Z.Q. Zhang, J.M. Fu, Distribution of particulate- and vapor-phase n-alkanes and polycyclic aromatic hydrocarbons in urban atmosphere of Guangzhou, China, Atmos. Environ. 37 (2003) 289–298.
[9] J. Li, G. Zhang, X.D. Li, S.H. Qi, G.Q. Liu, X.Z. Peng, Source seasonality of polycyclic aromatic hydrocarbons (PAHs) in a subtropical city, Guangzhou, South China, Sci.Total Environ. 355 (2006) 145–155.
[10] B. Gao, J.Z. Yu, S.X. Li, X. Ding, Q.F. He, X.M. Wang, Roadside and rooftop measurements of polycyclic aromatic hydrocarbons in PM2.5 in urban Guangzhou: evaluation of vehicular and regional combustion source contributions, Atmos. Environ. A: Gen. 45 (2011) 7184–7191.

[11] Y.L. Zhang, H. Guo, X.M. Wang, I.J. Simpson, B. Barletta, D.R. Blake, S. Meinardi, F.S. Rowland, H.R. Cheng, S.M. Saunders, S.H.M. Lam, Emission patterns and spatiotemporal variations of halocarbons in the Pearl River Delta region, southern China, J. Geophys. Res.: Atmos. 115 (2010).
[12] H. Guo, A.J. Ding, T. Wang, I.J. Simpson, D.R. Blake, B. Barletta, S. Meinardi, F.S. Rowland, S.M. Saunders, T.M. Fu, W.T. Hung, Y.S. Li, Source origins modeled profiles, and apportionments of halogenated hydrocarbons in the greater Pearl River Delta region, southern China, J. Geophys. Res.: Atmos. 114 (2009).
[13] H. Guo, F. Jiang, H.R. Cheng, I.J. Simpson, X.M. Wang, A.J. Ding, T.J. Wang, S.M. Saunders, T. Wang, S.H.M. Lam, D.R. Blake, Y.L. Zhang, M. Xie, Concurrent observations of air pollutants at two sites in the Pearl River Delta and the implication of regional transport, Atmos. Chem. Phys. 9 (2009) 7343–7360.
[14] NIOSH, Method 5040 issue 3 (interim): elemental carbon (diesel exhaust), in: NIOSH Manual of Analytical Methods, National Institute of Occupational Safety and Health, Cincinnati, OH, 1999.
[15] M.P. Fraser, K. Lakshmanan, Using levoglucosan as a molecular marker for the long-range transport of biomass combustion aerosols, Environ. Sci. Technol. 34 (2000) 4560–4564.
[16] B.R.T. Simoneit, Biomass burning – a review of organic tracers for smoke from incomplete combustion, Appl. Geochem. 17 (2002) 129–162.
[17] M.E. Birch, R.A. Cary, Elemental carbon-based method for monitoring occupational exposures to particulate diesel exhaust, Aerosol Sci. Technol. 25 (1996) 221–241.
[18] J.J. Schauer, W.F. Rogge, L.M. Hildemann, M.A. Mazurek, G.R. Cass, Source apportionment of airborne particulate matter using organic compounds as tracers, Atmos. Environ. 30 (1996) 3837–3855.
[19] Y.X. Zhang, J.J. Schauer, Y.H. Zhang, L.M. Zeng, Y.J. Wei, Y. Liu, M. Shao, Characteristics of particulate carbon emissions from real-world Chinese coal combustion, Environ. Sci. Technol. 42 (2008) 5068–5073.
[20] D.R. Oros, B.R.T. Simoneit, Identification and emission rates of molecular tracers in coal smoke particulate matter, Fuel 79 (2000) 515–536.
[21] Y.Y. Yang, P.R. Guo, Q. Zhang, D.L. Li, L. Zhao, D.H. Mu, Seasonal variation, sources and gas/particle partitioning of polycyclic aromatic hydrocarbons in Guangzhou, China, Sci. Total Environ. 408 (2010) 2492–2500.
[22] US Environmental Protection Agency, Provisional Guidance for Quantitative Risk Assessment of Polycyclic Aromatic Hydrocarbons, EPA/600/R-93/089, (1993).
[23] US Environmental Protection Agency, Integrated Risk Information System, Benzo[a]pyrene, (2001).
[24] International Agency for Research on Cancer, Overall Evaluations of Carcinogenicity to Humans, (2001).
[25] L.C. Marr, K. Dzepina, J.L. Jimenez, F. Reisen, H.L. Bethel, J. Arey, J.S. Gaffney, N.A. Marley, L.T. Molina, M.J. Molina, Sources and transformations of particle-bound polycyclic aromatic hydrocarbons in Mexico City, Atmos. Chem. Phys. 6 (2006) 1733–1745.
[26] N. Yassaa, B.Y. Meklati, A. Cecinato, F. Marino, Particulate n-alkanes, n-alkanoic acids and polycyclic aromatic hydrocarbons in the atmosphere of Algiers City Area, Atmos. Environ. 35 (2001) 1843–1851.
[27] A. Katsoyiannis, A.J. Sweetman, K.C. Jones, PAH molecular diagnostic ratios applied to atmospheric sources: a critical evaluation using two decades of source inventory and air concentration data from the UK, Environ. Sci. Technol. 45 (2011) 8897–8906.
[28] X. Ding, X.M. Wang, Z.Q. Xie, C.H. Xiang, B.X. Mai, L.G. Sun, M. Zheng, G.Y. Sheng, J.M. Fu, U. Poschl, Atmospheric polycyclic aromatic hydrocarbons observed over the North Pacific Ocean and the Arctic area: spatial distribution and source identification, Atmos. Environ. 41 (2007) 2061–2072.
[29] M.B. Yunker, R.W. Macdonald, R. Vingarzan, R.H. Mitchell, D. Goyette, S. Sylvestre, PAHs in the Fraser River basin: a critical appraisal of PAH ratios as indicators of PAH source and composition, Org. Geochem. 33 (2002) 489–515.
[30] L.Y. He, M. Hu, Y.H. Zhang, X.F. Huang, T.T. Yao, Fine particle emissions from on-road vehicles in the Zhujiang Tunnel, China, Environ. Sci. Technol. 42 (2008) 4461–4466.
[31] H.A. Yu, J.Z. Yu, Size distributions of polycyclic aromatic hydrocarbons at two receptor sites in the Pearl River Delta Region, China: implications of a dominant droplet mode, Aerosol Sci. Technol. 45 (2011) 101–112.
[32] R.J. Sheesley, J.J. Schauer, Z. Chowdhury, G.R. Cass, B.R.T. Simoneit, Characterization of organic aerosols emitted from the combustion of biomass indigenous to South Asia, J. Geophys. Res.: Atmos. 108 (2003).
[33] M. Zheng, L.G. Salmon, J.J. Schauer, L.M. Zeng, C.S. Kiang, Y.H. Zhang, G.R. Cass, Seasonal trends in PM2.5 source contributions in Beijing, China, Atmos. Environ. 39 (2005) 3967–3976.
[34] M. He, J.Y. Zheng, S.S. Yin, Y.Y. Zhang, Trends, temporal and spatial characteristics, and uncertainties in biomass burning emissions in the Pearl River Delta, China, Atmos. Environ. 45 (2011) 4051–4059.
[35] F. Fung, H. He, B. Sharpe, F. Kamakaté, K. Blumberg, Overview of China's Vehicle Emission Control Program, http://www.theicct.org/node/6 (2010).